Optimal design of inerter devices combined with TMDs for vibration control of buildings exposed to stochastic seismic excitations

L. Marian & A. Giaralis
City University London, United Kingdom

ABSTRACT: This paper proposes a novel configuration for the passive vibration control of seismically excited buildings combining the “inerter”, a recently developed two-terminal flywheel (TTF) device, with the classical tuned mass damper (TMD). The TTF is used as an inter-storey device acting as an “apparent mass amplifier” to the TMD mass to control the fundamental mode shape of planar framed buildings base excited by stationary stochastic processes. Pertinent numerical data reported establish that the use of the TTF in the proposed TMD+TTF configuration can either replace a considerable part of the TMD vibrating mass to achieve a significantly lighter passive vibration control solution, or improve the TMD performance for a fixed TMD mass. These data consider the mean square and the peak top floor displacement of a particular three-storey building frame equipped with optimally designed classical TMD and TMD+TTF passive control solutions for seismic input compatible with the response spectrum of the European aseismic code provisions (EC8).

1 INTRODUCTION

Civil engineering structures at seismically prone areas are exposed to earthquake induced ground motions of different severity levels during the structures’ life service. At high levels of seismic severity, the inertial dynamic loads exerted to structures may induce permanent damage and, in extreme cases, total structural failure/collapse. In fact, current codes of practice for earthquake resistance allow for ordinary structures to yield under a specified “design” seismic excitation level to reduce the initial construction cost (e.g. CEN 2004). However, recent major seismic events caused extensive structural damage in various metropolitan areas (e.g. Kobe-Japan 1995 and Christchurch-New Zealand 2011) where the associated cost of structural retrofit and downtime has been significant. In this respect, the incorporation of various devices such as base isolators, energy dissipation equipment (e.g. viscous dampers, friction dampers, etc.), and tuned-mass dampers (TMDs) has been proposed by various researchers and has been considered in practice to achieve “minimal damage” structures (e.g. Naeim & Kelly 1999, Chang 1999, Spencer 2002, Martelli & Forni 2011, Karavasilis et al. 2011). Such passive vibration control devices/equipment are designed to maintain the response of seismically excited structures under certain acceptable thresholds.

In this context, this paper considers the use of two-terminal flywheel (TTF) devices, originally introduced by Smith (2002), for the passive vibration control of building structures exposed to the earthquake hazard. In its ideal form, a TTF device, or the “inerter” as is referred to in Smith (2002), has two terminals free to move independently and develops an internal (resisting) force proportional to the relative acceleration of its terminals. In Figure 1, a ‘black-box’ representation of a TTF/inerter is shown whose terminals are subject to an equal and opposite externally applied force F in equilibrium with the internally developed force. By definition of the inerter the following relationship holds (Smith 2002, Chuan et al. 2011a)

$$F = b(\ddot{x}_1 - \ddot{x}_2), \qquad (1)$$

where x_1 and x_2 are the displacement coordinates of the two terminals and a dot over symbol signifies differentiation with respect to time. In the above equation, the constant of proportionality b has mass units and fully characterizes the behavior of the device.

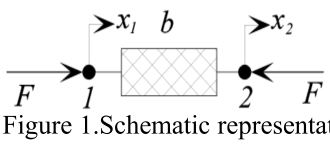

Figure 1.Schematic representation of the two-terminal flywheel device (b is the mass-equivalent constant of proportionality)

Employing rack and pinion gearing arrangements to drive a rotating flywheel, some TTF prototypes have been physically built (Smith 2002, Chuan et al.

2011a). In fact, TTF devices/inerters have been successfully used for vibration control of suspension systems in high performance vehicles (e.g. Evangelou et al. 2004, Chuan et al. 2011b). However, thus far, relatively limited work has been reported in the open literature exploring the potential of TTFs for passive vibration control of civil engineering structures. In particular, the performance of "suspension control" for civil structures employing inerters in a "base isolation" kind of arrangement has been studied by Wang et al. (2007) and by Wang et al. (2010): they establish that TTFs are effective in controlling the response of the rigid superstructure exposed to vertical band-limited white noise ground motions. Furthermore, a number of energy dissipation devices combining an apparent "mass amplifier", which achieves a similar dynamic effect as the TTF/inerter, in parallel with a viscous damper have been discussed in the literature (Hwang et al. 2007, Ikago et al. 2012). These rotational inertia dampers are usually arranged as diagonal bracing members in multi-storey framed buildings to provide supplemental damping and inertia properties to structures (e.g. Ikago et al. 2011). In this manner, passive control of seismically excited buildings is achieved by increase of the inherent to all structures damping and mass properties.

Herein, a novel study is undertaken considering the use of TTF devices in conjunction with the classical Tuned Mass Damper (TMD) for passive vibration control of buildings exposed to horizontal strong ground motions. In its simplest form, the TMD involves an attached mass m_{TMD} to the structure whose vibration motion is to be controlled (primary structure) via a linear spring and a viscous damper with stiffness coefficient k_{TMD} and damping coefficient c_{TMD}, respectively. It relies on "tuning" the k_{TMD} and c_{TMD} properties for a specified m_{TMD} such that significant kinetic energy is transferred from the vibrating primary structure to the TMD mass and is "absorbed" at the damper (e.g. Ayorinde & Warburton 1980, Lee et al. 2006, Hoang et al 2008). In the case of "regular" multi-storey buildings, the TMD mass can be attached to the top floor to suppress the buildings' oscillatory motion according to its fundamental mode shape (e.g. Rana and Soong 1998). This mass is quite substantial commonly ranging in between 1% to 10% of the total mass of the building.

In this regard, it is herein proposed to consider the TTF as an inter-story connective device placed in a 'diagonal' configuration between the TMD mass, located at the top floor, and the second to the top floor mass in multi-storey frame buildings as shown in Figure 2. The proposed passive vibration control configuration is motivated by the fact that a TTF device of approximately 1 kg of physical mass may be built to attain a constant of proportionality b in the range of 60–200 kg depending on the size of the flywheel (Papageorgiou & Smith 2005). Thus, the aim is to exploit the mass amplifying effect of the inerter to either reduce the TMD mass necessary to achieve a certain level of vibration control, or to enhance the performance of the TMD for a fixed m_{TMD} value.

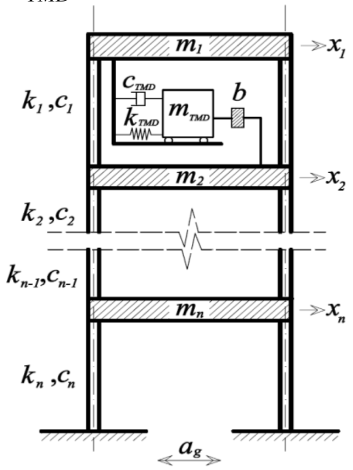

Figure 2. N-storey building with a TMD at the top floor and an inter-story TTF device.

Note that, in this study, the primary structure is assumed to behave linearly in alignment with current trends in performance based requirements for minimally damaged structures protected by passive control devices. Further, the seismic input excitation considered in the optimum design of the proposed "TMD+TTF" configuration is modeled via a stationary stochastic process.

The remainder of this paper is organized as follows: In section 2 the governing equations of motions for the proposed "TMD+TTF" configuration are derived. Section 3 presents a procedure for optimum design of the TMD+TTF system for a stochastically base-excited primary structure. Section 4 provides numerical data to demonstrate the effectiveness and applicability of the proposed passive vibration control solution vis-à-vis the classical TMD. Section 5, summarizes the main conclusions of the work.

2 GOVERNING EQUATIONS OF MOTION

Consider the n-story planar frame ("primary structure") of Figure 2, equipped with the herein proposed TMD-TTF passive vibration control configuration and base excited by a horizontal acceleration process a_g. For the purposes of this study, the considered primary structure is modeled as a proportionally damped multi-degree-of-freedom (MDOF) system with masses m_i (i=1,2,…n) lumped at each floor, and with k_i and c_i being the lateral stiffness and damping coefficient of each storey. The n+1 equations of motion of this MDOF system can be written in matrix form as

$$[M]\{\ddot{X}\} + [C]\{\dot{X}\} + [K]\{X\} = -[M]\{\delta\}a_g, \qquad (2)$$

where $\{\delta\}$ is the unit column vector, and $\{X\}$ is the vector collecting all lateral floor deflections x_i plus the relative to the ground displacement x_{TMD} of the attached mass of the TMD. That is,

$$\{X\} = \{x_{TMD}(t)\ x_1(t)\ \ x_2(t)\ \ \cdots\ x_n(t)\}^T, \quad (3)$$

where the superscript "T" denotes matrix transposition. Further, in Equation 1 the mass matrix $[M]$, the damping matrix $[C]$, and the stiffness matrix $[K]$ are given, respectively, as

$$[M] = \begin{bmatrix} m_{TMD}+b & 0 & -b & 0 & \cdots & 0 \\ 0 & m_1 & 0 & 0 & \cdots & \vdots \\ -b & 0 & m_2+b & 0 & \cdots & \vdots \\ 0 & 0 & 0 & m_3 & \cdots & \vdots \\ \vdots & \vdots & \vdots & \vdots & \ddots & 0 \\ 0 & \cdots & \cdots & \cdots & 0 & m_n \end{bmatrix},$$

$$[C] = \begin{bmatrix} c_{TMD} & -c_{TMD} & 0 & \cdots & 0 \\ -c_{TMD} & c_1+c_{TMD} & -c_1 & 0 & \vdots \\ 0 & -c_1 & c_1+c_2 & -c_2 & \vdots \\ 0 & 0 & -c_2 & \ddots & 0 \\ \vdots & \vdots & \vdots & \vdots & -c_{n-1} \\ 0 & \cdots & 0 & -c_{n-1} & c_{n-1}+c_n \end{bmatrix}, \quad (4)$$

$$[K] = \begin{bmatrix} k_{TMD} & -k_{TMD} & 0 & \cdots & 0 \\ -k_{TMD} & k_1+k_{TMD} & -k_1 & 0 & \vdots \\ 0 & -k_1 & k_1+k_2 & -k_2 & \vdots \\ 0 & 0 & -k_2 & \ddots & 0 \\ \vdots & \vdots & \vdots & \vdots & -k_{n-1} \\ 0 & \cdots & 0 & -k_{n-1} & k_{n-1}+k_n \end{bmatrix}.$$

Note that for $b=0$ Equations 2-4 correspond to the case of a primary structure equipped with the classical TMD attached to the top floor. This TMD topology is used to control the first mode of vibration which, for "regular" in elevation frames, will dominate their dynamic response to broadband earthquake excitations (e.g. Rana & Soong 1998). The inclusion of the TTF device according to the proposed configuration alters the mass matrix which is no longer diagonal. However, the overall structural system remains linear and, from a practical viewpoint, the well established in the literature methods for optimal TMD design can be readily applied (e.g. Rana & Soong 1998, Hoang et al. 2008, Salvi & Rizzi 2011). The following section briefly reviews the steps taken for optimum design of the herein TMD-TTF configuration for a given primary structure and for pre-specified (fixed) values of m_{TMD} and b.

3 OPTIMUM DESIGN OF PROPOSED TMD-TTF CONFIGURATION FOR STOCHASTIC SEISMIC EXCITATION

Let ω_{TMD} and ξ_{TMD} be the natural frequency and the critical damping ratio of the TMD, respectively, defined as

$$\omega_{TMD} = \sqrt{\frac{k_{TMD}}{m_{TMD}}} \quad and \quad \xi_{TMD} = \frac{c_{TMD}}{2m_{TMD}\omega_{TMD}}. \quad (5)$$

Further, consider the dimensionless modal mass ratio μ_M and frequency ratio υ defined by

$$\mu_M = \frac{m_{TMD}}{M_1} \quad \text{and} \quad \upsilon = \frac{\omega_{TMD}}{\omega_1}, \quad (6)$$

where M_1 is the generalized mass of the fundamental mode shape of the uncontrolled (primary) structure given by the expression

$$M_1 = \{\Phi_{1n}\}^{\mathrm{T}}[M_p]\{\Phi_{1n}\}. \quad (7)$$

In the last equation $\{\Phi_{1n}\}$ is the fundamental mode shape vector (eigenvector) normalized with respect to its first element corresponding to the DOF of the top floor (see also Rana & Song 1998). Further, $[M_p]$ is obtained from the mass matrix $[M]$ of Equation (4) by elimination of the first row and column and by setting b equal to zero.

In this study, the input seismic excitation is modeled by a stationary stochastic process represented in the frequency domain by a power spectral density function $S(\omega)$. Optimal design values for the frequency ratio υ, the damping ratio ξ_{TMD} are sought to minimize the mean square displacement of the top floor of the primary structure given the properties of the primary structure, the modal mass ratio μ_M, and the TTF coefficient b. In particular, the following non-dimensional performance index (PI) is considered in the optimization problem (cost function)

$$PI = J^{TMD+TTF}/J^0, \quad (8)$$

where (see also Hoang et al. 2008)

$$J^{TMD+TTF} = \int_0^\infty |G_1(\omega)|^2 S(\omega)\, d\omega. \quad (9)$$

In the last equation, $|G_1(\omega)|^2$ represents the squared modulus of the frequency response function ("transfer function") between the seismic input and the top floor displacement of the primary structure. This function is defined in the Appendix A for the special case of a three-storey primary structure equipped with the "TMD+TTF" configuration of Figure 2. Further, in Equation 8, J^0 denotes the variance of the top floor displacement for the uncontrolled primary (linear) structure exposed to the input seismic action represented by $S(\omega)$. Note that notation-wise for b=0: $J^{TMD+TTF}= J^{TMD}$ and for $b=\mu_M=0$: $J^{TMD+TTF}=J^0$.

In all of the ensuing numerical examples a MATLAB® built-in "min-max" constraint optimization algorithm employing a sequential programming method is used to minimize the PI of Equation (8) for the design parameters υ and ξ_{TMD} (see also Salvi & Rizzi 2011). The following expressions are used to obtain initial estimates of the sought optimum design values used as "seed" values to the adopted optimization algorithm

$$\upsilon = \frac{\sqrt{1-\mu_M/2}}{1+\mu_M} \quad \text{and} \quad \xi_{TMD} = \sqrt{\frac{\mu_M(1-\mu_M/4)}{4(1+\mu_M)(1-\mu_M/2)}}. \quad (10)$$

The above formulae yield optimum design TMD parameters which minimize J^{TMD} for an undamped linear single-DOF primary structure under white noise excitation (Ayorinde & Warburton, 1980). As a final note, appropriate constraints are imposed to the sought design parameters relying on physical considerations.

4 NUMERICAL APPLICATION FOR EC8 COMPATIBLE SEISMIC EXCITATION

4.1 *Derivation of optimal design parameters*

In this section optimum design parameters are derived following the procedure reviewed in section 3 for the TMD+TTF passive vibration control solution of Figure 2. A three-story primary structure is considered whose inertial and elastic properties are collected in Table 1. Table 2 reports the undamped natural frequencies of the considered primary structure obtained from standard modal analysis. Further, the 3-by-3 damping matrix of the (uncontrolled) primary structure $[C_p]$ is assumed to be proportional to the stiffness matrix of the primary structure $[K_p]$ following the expression

$$[C_p] = \frac{2\xi_1}{\omega_1}[K_p], \tag{11}$$

where ω_1 is the fundamental undamped natural frequency of the primary structure and ξ_1 is the critical damping ratio of the fundamental mode shape taken equal to 0.02. In the last equation $[K_p]$ is obtained from the stiffness matrix $[K]$ of Equation (4) by elimination of the first row and column and by setting k_{TMD} equal to zero.

Table 1. Inertial and elastic properties of the considered three-storey primary structure

Storey	Mass (kg)	Stiffness (N/m)
1 (top)	10 x 10^3	10 x 10^5
2	15 x 10^3	25 x 10^5
3	20 x 10^3	35 x 10^5

Table 2. Undamped natural frequencies of the considered three-storey primary structure.

Mode	1st	2nd	3rd
Period (s)	1.00	0.48	0.31
Frequency (rad/s)	6.37	13.02	20.57

The input seismic action is represented by the stationary power spectrum $S(\omega)$ plotted in Figure 3b which is compatible in the "mean sense" with the elastic spectrum of the current European aseismic code provisions (EC8) for peak ground acceleration 0.36g (g=981cm/s^2) and ground type "B" (gray thick line in Figure 3a) (CEN 2004). The considered power spectrum is derived by a methodology described in detail in Giaralis and Spanos (2010). Median spectral ordinates of an ensemble of 1000 20s long stationary signals compatible with the power spectrum of Figure 3b are included in Figure 3a to ensure numerically the "mean sense" compatibility achieved by $S(\omega)$ with respect to the considered EC8 spectrum. These signals have been generated using a random field simulation technique based on an auto-regressive-moving-average filter (e.g. Giaralis & Spanos 2009).

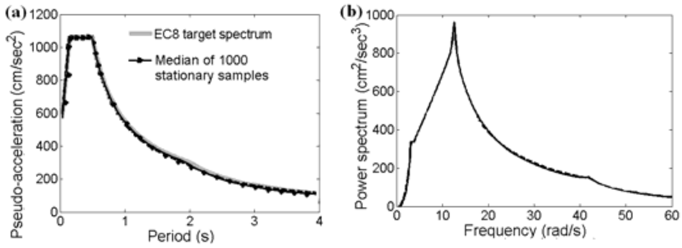

Figure 3. Considered EC8 compatible power spectrum $S(\omega)$ for design purposes

In what follows, the optimization procedure of section 3 is applied to derive optimum design parameters υ and ξ_{TMD} for the considered three-storey primary structure, the input power spectrum of Figure 3b and for various values of μ_M and b.

4.1.1 *Optimum TMD (b=0) design parameters*

The normalized by the top floor value of the first mode shape vector of the considered primary structure is computed as $\{\Phi_{1n}\}=\{1\ \ 0.5934\ \ 0.286\}^T$. The corresponding generalised mass is computed from Equation 7 as M_1= 16.9x10^3 kg. Setting the mass of the TMD equal to 450 kg, that is 1% of the total mass of the primary structure, the modal mass ratio becomes μ_M= 0.0267. The latter value is, next, substituted in Equations 10 to obtain the seed values (υ= 0.967 and ξ_{TMD}= 0.081) used as input to the adopted optimization algorithm. Figure 4 plots the derived optimum parameters (frequency ratio υ and damping ratio ξ_{TMD}) for the particular case considered. Similar computations are performed for a wide range of assumed m_{TMD} values commonly used in civil engineering applications: from 1% to 10% of the total mass of the primary structure, which corresponds to 225kg to 4500kg in the particular case considered. Numerical results obtained from the adopted optimization procedure are plotted in terms of the "free" TMD design parameters (υ and ξ_{TMD}) in Figure 4 and in terms of the PI of Equation 9 in Figure 5.

The numerical data presented in Figures 4 and 5 are in alignment with similar results reported in the literature obtained by alternative numerical optimization techniques (see e.g. Lee et al. 2006, Hoang et al. 2008, Salvi and Rizzi 2011 and references therein). Specifically, increased values of the assumed TMD mass necessitate higher ξ_{TMD} values and lower TMD frequency ratios to achieve optimal tuning. Further, larger values for the TMD mass are more effective in controlling the dynamic response of the primary structure related to its fundamental (and dominant) mode shape. However, the rate of decrease of the PI decreases rapidly (PI "saturates") as the TMD mass increases. It reaches an almost flat plateau for m_{TMD} values larger than 5% the total mass of the considered primary structure.

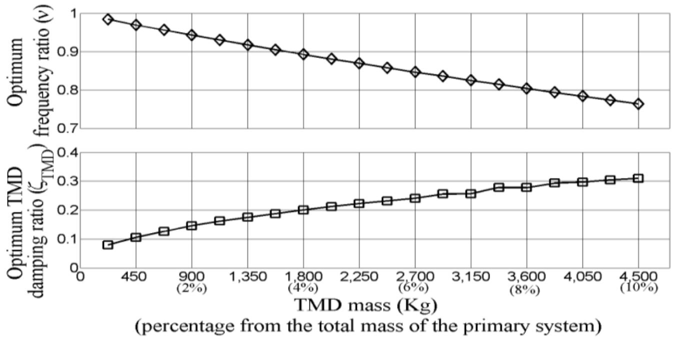

Figure 4. Optimum TMD frequency ratio and TMD damping ratio versus the TMD mass (*b=0*)

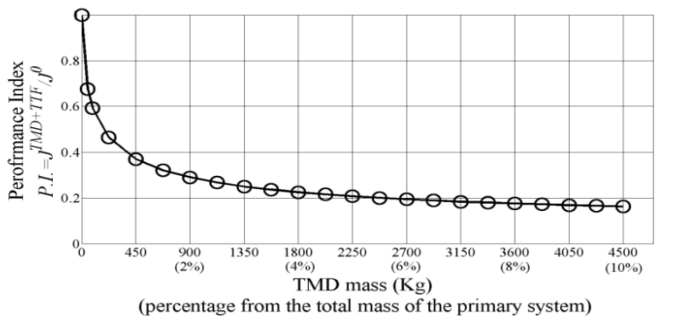

Figure 5. Performance index versus the TMD mass (*b=0*)

4.1.2 *Optimum TMD with TTF (b>0) design parameters*

A TTF/inerter device is incorporated to the considered three-story primary structure according to the proposed configuration of Figure 2 (see also Appendix A). The previously described optimization procedure is used to derive optimum TMD parameters for the same range of pre-specified TMD mass values and for several values of the TTF constant *b*. For each value, the optimisation procedure described in section 3 is repeated. Obtained numerical data are plotted in Figure 6 in terms of the "free" TMD design parameters (υ and ξ_{TMD}) and in Figure 7 in terms of the PI of Equation 9. The data of Figures 4 and 5 corresponding to the TMD system (*b*=0) are also included in Figures 6 and 7, respectively, for the sake of comparison. Further, the same data are provided in tabular form, as well (Table 3).

It can be readily deduced from the reported numerical data that the proposed TMD+TTF configuration reduces the value of the Performance Index (top floor response variance) as the value of the TTF *b* increases. In all cases, the proposed model outperforms the classical TMD in terms of minimizing the adopted cost function. The performance improvement is more dramatic for relatively small TMD mass values (less than about 3% of the total mass of the primary structure) while it becomes insignificant for TMD mass values greater than 6% of the total mass of the primary structure. However, it is noted that this enhanced performance comes at the cost of higher damping and stiffness values for the elements connecting the TMD mass to the primary structure.

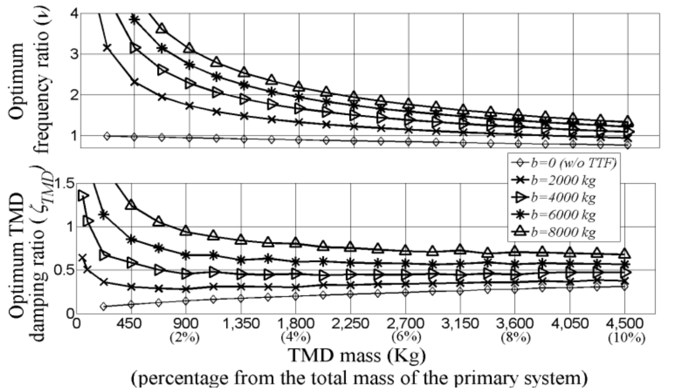

Figure 6. Optimum TMD frequency ratio and TMD damping ratio versus the TMD mass for various values of *b*.

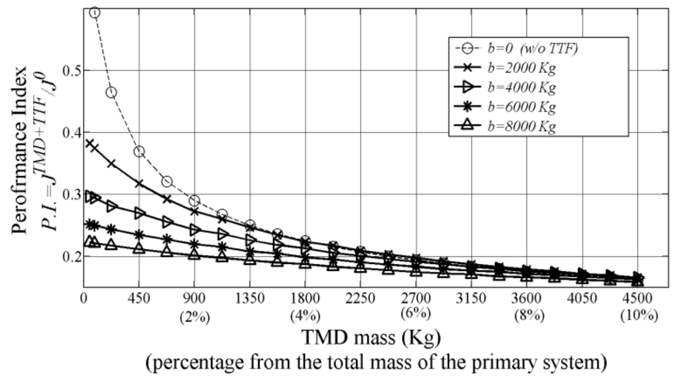

Figure 7. Performance index versus the TMD mass for various values of *b*.

Table 3. TMD parameters and Performance Index for different values of the TMD mass and of the TTF constant b.

m_{TMD} (kg)	b (kg)	υ	ξ_{TMD}	PI	Improvement (%)
450 (1%)	0(w/o TTF)	0.97	0.105	0.369	-
	2000	2.31	0.307	0.317	14.1
	4000	3.16	0.582	0.270	27.0
	6000	3.84	0.852	0.235	36.5
	8000	4.42	1.241	0.211	42.8
900 (2%)	0(w/o TTF)	0.94	0.146	0.290	-
	2000	1.73	0.280	0.272	6.1
	4000	2.28	0.454	0.243	16.3
	6000	2.73	0.671	0.220	24.4
	8000	3.12	0.938	0.201	30.7
1350 (4%)	0(w/o TTF)	0.92	0.175	0.250	-
	2000	1.48	0.310	0.246	1.4
	4000	1.89	0.452	0.226	9.5
	6000	2.24	0.615	0.208	16.8
	8000	2.53	0.840	0.193	22.6
1800 (6%)	0(w/o TTF)	0.89	0.200	0.225	-
	2000	1.32	0.301	0.224	0.6
	4000	1.66	0.455	0.213	5.4
	6000	1.94	0.594	0.198	11.8
	8000	2.17	0.803	0.187	16.7

More importantly, the herein furnished data demonstrates the applicability of using the "mass amplifying" effect of the TTF/inerter device to replace part of the oscillating mass of the TMD. This may be a significant advantage in certain real-life earthquake resistance design scenarios. For example, in the case of the herein considered primary structure and EC8 compatible seismic excitation, the use of a TTF/inerter with a "mass" constant of b=8000 kg in combination with a TMD mass of 900kg achieves similar level of response in terms of top floor deflection variance as the classical TMD three times heavier oscillating mass (2700kg). However, the physical mass of the employed inerter might be up to two orders of magnitude smaller than its b constant, that is, about 100 kg (Papageorgiou & Smith 2005). Thus, the total weight of the examined TTF+TMD system becomes three times lighter than the classical TMD.

4.2 *Performance assessment for field recorded EC8 compatible accelerograms*

This section furnishes further numerical results to quantify the effectiveness of the herein proposed TMD+TTF configuration vis-à-vis the classical TMD for passive vibration control of building structures. To this aim, the peak top floor deflection of the previously described three-storey primary structure equipped with a TMD with $m_{TMD}=900\ kg$ and of a TMD+TTF with $m_{TMD}=900\ kg$ and $b=8000\ kg$ is obtained for an ensemble of 7 field recorded accelerograms (Table 4). The two considered passive vibration control systems have been optimally designed for the stochastic input compatible with the EC8 spectrum of Figure 3 as detailed in the previous section (see also Table 3). The top row of Table 4 reports the obtained properties for the two systems using Equations 5. Further, the same Table lists the considered 7 accelerograms: they have been selected out of a data-bank specifically proposed to be used as input for the design and assessment of passively controlled civil structures (Naeim & Kelly 1999). The original records have been scaled in a non-uniform manner using a harmonic wavelet-based approach (Giaralis & Spanos 2009, Giaralis & Spanos 2010a) to become compatible with the target EC8 spectrum of Figure 3a according to EC8 compatibility criteria. Specifically, their average response spectral ordinates are greater than 90% of the target spectrum within a $[0.2T_1\ 2T_1]$ period interval where T_1=1s is the fundamental natural period of the considered primary structure (Figure 8). This numerical study is motivated by the fact that EC8 prescribes using the *average* of pertinent peak response quantities for design purposes when at least 7 response history analyses are performed for spectrum compatible accelerograms.

On average (Table 4), the TMD (b=0) achieves 80% peak response reduction compared to the uncontrolled primary structure, while the TMD+TTF achieves 60% reduction. This significant additional peak response reduction accomplished by the herein proposed configuration is due to the virtual "mass amplifying effect" of the TTF which can accommodate, in an optimal manner, a damper with an order of magnitude higher damping coefficient (c_{TMD}) for the same m_{TMD} mass. However, as previously mentioned, the added actual mass of the TTF in this case is of the order of 100kg.

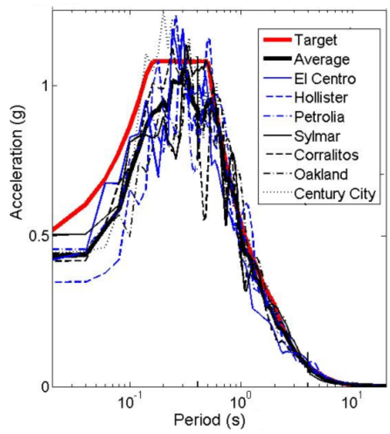

Figure 8. Response spectra of the considered EC8 compatible field recorded accelerograms listed in Table 4.

Table 4. Maximum top floor displacements (cm)

Recorded strong ground motion component	Primary structure	Optimal TMD m_{TMD}= 900kg k_{TMD}= 32.5kN/m c_{TMD}= 1.57kNs/m	Optimal TMD+TTF b=8000kg m_{TMD}= 900kg k_{TMD}= 355.5kN/m c_{TMD}= 33.5kNs/m
Petrolia- 90° 1992- Petrolia	24.25	21.27	15.70
Corralitos- 90° Eureka Canyon 1989-Loma Prieta	23.45	17.36	14.87
El Centro #6-230° Huston Rd. 1979-Imperial Val.	27.96	20.31	15.94
Hollister-90° South St & Pine Dr 1989- Loma Prieta	27.67	20.32	14.16
Oakland-35° Outer harbor wharf 1989- Loma Prieta	26.02	23.35	16.91
Century City-90° LACC North (1994- Northridge)	23.12	18.78	13.54
Sylmar- 90° County Hospital (1994- Northridge)	24.35	20.11	16.38
Average	**25.26**	**20.22**	**15.36**

The beneficial effect of adding the TTF to the classical TMD in the proposed configuration to control the top floor displacement is demonstrated in Figure 10 which plots the top floor time history displacement of the primary structure exposed to the Sylmar accelerogram of Figure 9. These are obtained by standard numerical integration of the linear equations of motion for the uncontrolled and the two controlled cases considered in Table 4. The proposed TMD-TTF configuration controls better the displacement throughout the duration of the strong ground motion. Similar conclusions are drawn from response histories obtained for the other 6 EC8 compatible accelerograms not included here for the sake of brevity.

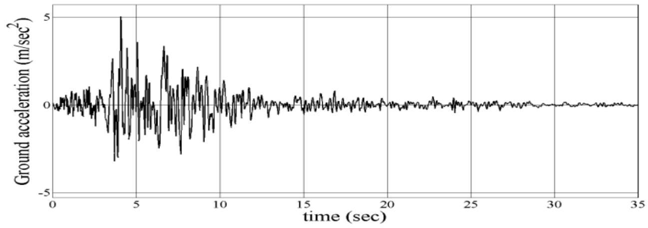

Figure 9. Wavelet-based modified Sylmar- 90°, County Hospital parking lot component- Northridge 1994 earthquake.

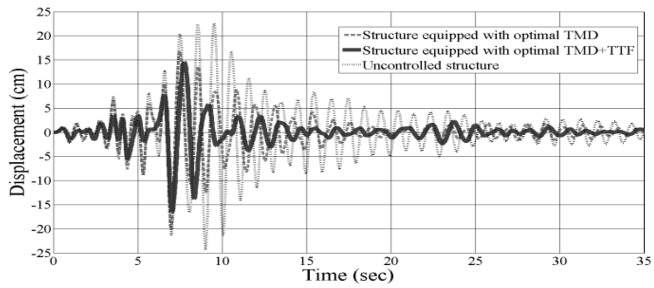

Figure 10. Top floor displacement responses for uncontrolled structure, structure equipped with optimal TMD and structure equipped with optimal TMD and TTF device.

5 CONCLUDING REMARKS

A novel configuration for the passive vibration control of seismically excited buildings have been proposed combining the "inerter", a recently developed two-terminal flywheel (TTF) device, with the classical tuned mass damper (TMD). In particular, the TTF is used as an inter-storey device acting as an "apparent mass amplifier" to the TMD mass. The equations of motion of a linear damped multi degree-of-freedom frame primary structure equipped with the proposed TMD+TTF configuration to control the fundamental mode of vibration have been derived. It has been demonstrated that the considered configuration can be viewed as a generalization of the classical TMD. Thus, all established in the literature procedures for optimum TMD tuning/design are readily applicable for the new TMD+TTF configuration, as well. A min-max optimization procedure has been considered to obtain optimum TMD and TMD+TTF parameters which minimize the mean square top floor displacement of a three-story frame building base excited by a stationary stochastic process. An input stochastic process compatible with the elastic design spectrum of the European aseismic code provisions (EC8) has been assumed. The thus derived numerical data evidence that the TTF used in the proposed configuration can either replace part of the TMD vibrating mass to achieve a significantly lighter passive vibration control solution (TMD mass replacement potential), or improve the TMD performance for a fixed TMD mass (TMD mass amplification effect). The latter effect is more significant for relatively small TMD masses where the inclusion of the TTF allows for efficiently/optimum usage of dampers with much higher damping coefficients compared to an optimally tuned classical TMD.

Furthermore, the effectiveness of the proposed TMD+TTF configuration over the classical TMD has been demonstrated by performing response history analyses for an ensemble of 7 EC8 spectrum compatible field recorded strong ground motions. The optimally tuned TMD+TTF solution achieved considerable reduction of the peak average top floor displacement of the considered three-storey building compared to the one achieved by the optimally designed classical TMD assuming the same TMD mass in both cases.

Overall, the herein reported numerical data provide evidence that the use of a TTF as an interstorey device in conjunction with the TMD offers a novel promising solution for passive vibration control of building structures. Further on-going work by the authors is directed towards establishing alternative configurations/topologies to combine TMDs with TTF devices to control the dynamic response of various civil structures for stochastic and deterministic excitations and for various response minimization criteria.

APPENDIX A

The modeling assumptions of section 2 for the primary building structure allow for its representation as a linear chain-like spring-mass-damper system. Thus, the proposed TMD+TTF configuration can be studied by means of passive mechanical admittances Q defined as the ratio of force over velocity (Hixson 1961). This is a common practice in topology studies of mechanical system networks. Figure 11 models the considered in section 4 three-storey primary structure with a TMD+TTF passive system. In particular, Q_1, Q_2, Q_3 are the mechanical admittances of the stiffness+damping "networks" connecting the three floor masses, Q_{TMD} is the mechanical admittance of the network that connects the top floor mass to the mass of the TMD and Q_{TTF} is the mechanical admittance of the network that connects the mass of the TMD to the second floor mass.

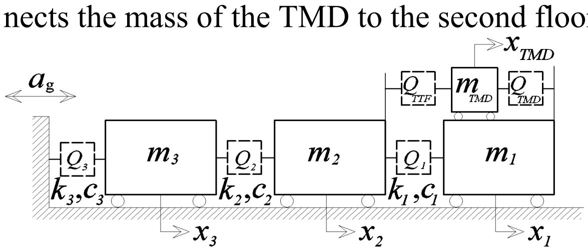

Figure 11. Equivalent mechanical model of the proposed frame structure. Mechanical admittance formulation.

Denoting the Laplace transform variable by s, the above mechanical admittances are expressed as:

$$Q_1(s) = \frac{k_1}{s} + c_1, Q_2(s) = \frac{k_2}{s} + c_2, Q_3(s) = \frac{k_3}{s} + c_3,$$
$$Q_{TMD}(s) = \frac{k_{TMD}}{s} + c_{TMD}, \quad \text{and} \quad Q_{TTF}(s) = bs \tag{12}$$

Next, Equation 2 can be written in the Laplace domain as

$$[B]\{\tilde{X}\} = -[M]\{\delta\}\widetilde{\mathrm{A}}, \tag{13}$$

where $\{\tilde{X}\}$ is the vector collecting the Laplace transformed elements of $\{X\}$, $\widetilde{\mathrm{A}}$ is the Laplace transform of a_g and the $[B]$ matrix is given as

$$\begin{bmatrix} m_1 s^2 + [Q_1(s) + Q_{TMD}(s)]s & -Q_1(s)s & 0 & -Q_{TMD}(s) \\ -Q_1(s)s & m_2 s^2 + [Q_1(s) + Q_2(s) + Q_{TTF}(s)]s & -Q_2(s)s & -Q_{TTF}(s) \\ 0 & -Q_2(s)s & m_3 s^2 + [Q_2(s) + Q_3(s)]s & 0 \\ -Q_{TMD}(s) & -Q_{TTF}(s) & 0 & m_{TMD}s^2 + [Q_{TMD}(s) + Q_{TTF}(s)]s \end{bmatrix} \tag{14}$$

Using Equation 13, the overall system transfer function given by

$$G_1(s) = \frac{\tilde{x}_1(s)}{\widetilde{\mathrm{A}}(s)}, \tag{15}$$

can be analytically derived. The latter relates the input base excitation with the output top-storey displacement. Evaluation of $G_1(s)$ along the imaginary axis ($s=\omega\sqrt{-1}$), yields the frequency response function $G(\omega)$ appearing in Equation 9.

REFERENCES

Ayorinde, E.O. & Warburton, G.B. 1980. Minimizing structural vibrations with absorbers, *Earthquake Engineering and Structural Dynamics*, 8:219–36.

CEN. (2004), Eurocode 8: Design of Structures for Earthquake Resistance – Part 1: General Rules, Seismic Actions and Rules for Buildings. EN 1998-1: 2004 E. Comité Européen de Normalisation, Brussels.

Chang, C.C. 1999. Mass dampers and their optimal designs for building vibration Control, *Engineering Structures*, 21:454–463.

Chuan, L., Liang, M., Wang, Y. & Dong, Y. 2011a. Vibration suppression using two terminal flywheel. Part I: Modeling and Characterization, *Journal of Vibration and Control*, 18(8):1096-1105.

Chuan, L., Liang, M., Wang, Y. & Dong, Y. 2011b. Vibration suppression using two terminal flywheel. Part II: application to vehicle passive suspension, *Journal of Vibration and Control*, 18(8):1353-1365.

Evangelou, S., Limebeer, D.J.N., Sharp, R.S. & Smith, M.C. 2004. Steering compensation for high-performance motorcycles, *In IEEE Conference on Decision and Control*, 43:749-754.

Giaralis, A. & Spanos, P.D. 2009. Wavelets based response spectrum compatible synthesis of accelerograms- Eurocode application (EC8), *Soil Dynamics and Earthquake Engineering*, 29: 219-235.

Giaralis, A. & Spanos, P.D. 2010a. Effective linear damping and stiffness coefficients of nonlinear systems for design spectrum based analysis, *Soil Dynamics and Earthquake Engineering*, 30: 798-810.

Giaralis, A. & Spanos, P.D. 2010b. Derivation of Eurocode 8 spectrum-compatible time-histories from recorded seismic accelerograms via harmonic wavelets, *In: Proceedings of the 9th HSTAM International Congress on Mechanics,* paper #23, pp. 669-677.

Hixson, E.L. 1961. Mechanical Impedance and Mobility, chap. 10. In C. M. Harris & A.G. Piersol (eds.), *Shock and Vibration Handbook, 5th ed., McGraw-Hill Book Company, Inc*., New York.

Hoang, N., Fujino, Y. & Warnitchai, P. 2008. Optimal tuned mass damper for seismic applications and practical design formulas, *Engineering Structures*, 30: 707-715.

Hwang, J-S., Kim, J. & Kim, Y-M. 2007. Rotational inertia dampers with toggle bracing for vibration control of a building structure. *Engineering Structures*, 29: 1201-1208.

Ikago, K., Sugimura, Y., Saito, K. & Inoue, N. 2011. Seismic displacement control of multiple-degree-of-freedom structures using tuned viscous mass dampers, In: *Proceedings of the 8th International Conference on Structural Dynamics, Eurodyn, Leuven, Belgium, 4-6 July 2011,* pp. 1800-1807 (ISBN 978-90-760-1931-4).

Ikago, K., Saito, K. & Inoue, N. 2012. Seismic control of single-degree-of-freedom structure using tuned viscous mass damper, *Earthquake Engineering and Structural Dynamics,* 41:453-474.

Karavasilis, T.L., Kerawala, S & Hale, E. 2011. Hysteretic model for steel energy dissipation devices and evaluation of a minimal-damage seismic design approach for steel buildings, *Journal of Constructional Steel Research*, 70:358-367.

Lee, C.L., Chen, Y.T., Chung, L.L. & Wang, Y.P. 2006. Optimal design theories and applications of tuned mass dampers, *Engineering Structures*, 28:43–53.

Martelli, A. & Forni, M. 2011. Seismic isolation and other passive anti-seismic systems: worldwide application and conditions for their correct use, In: *Proceedings of the 8th nternational Conference on Structural Dynamics, Eurodyn, Leuven, Belgium, 4-6 July 2011,* pp. 1750-1757 (ISBN 978-90-760-1931-4).

Naeim, F. & Kelly, J.M. 1999. *Design of Seismic Isolated Structures: from Theory to Practice*. New York: John Wiley and Sons.

Papageorgiou, C. & Smith, M.C. 2005. Laboratory experimental testing of inerters, *In: IEEE Conference on Decision and Control*, 44:3351-3356.

Rana, R. & Soong, T.T. 1998. Parametric study and simplified design of tuned mass dampers, *Engineering Structures*, Vol. 20(3):193-204.

Salvi, J. & Rizzi, E. 2011. Minimax optimization of Tuned Mass Dampers under seismic excitation, *International Conference on Structural Dynamics, Eurodyn*, 8:1892-1899.

Smith, M.C. 2002. Synthesis of mechanical networks: The Inerter, *IEEE Transactions on Automatic Control*, 47(10): 1648-1662.

Spencer, B.F.Jr. 2002. Supplemental Energy Dissipation: State-of-the-art and State-of-the practice, *Engineer Structures*, 24:243- 259.

Wang, F.-C., Chen, C.-W., Liao, M.-K. & Hong, M.-F. 2007. Performance Analyses of Building Suspension Control with Inerters, *IEEE Conference on Decision and Control*, 46: 3786-3791.

Wang, F-C., Chen, C.-W. & Hong, M.-F. 2010. Building Suspensions with Inerters, *Proceedings of the Institution of Mechanical Engineers, Part C: Journal of Mechanical Engineering Science*, 224: 1605-1616.